Earth Systems and Environment (2018) 2:5–14
https://doi.org/10.1007/s41748-018-0041-2

ORIGINAL ARTICLE

Histidine at Position 195 is Essential for Association of Heme-*b* in Lcp1$_{VH2}$

Sylvia Oetermann[1] · Robin Vivod[1] · Sebastian Hiessl[1] · Jens Hogeback[2] · Michael Holtkamp[2] · Uwe Karst[2] · Alexander Steinbüchel[1,3]

Received: 26 October 2017 / Accepted: 15 March 2018 / Published online: 26 March 2018

Abstract
The latex clearing protein (Lcp) is the key enzyme of polyisoprene degradation in actinomycetes (Yikmis and Steinbüchel in Appl Environ Microbiol 78:4543–4551, https://doi.org/10.1128/AEM.00001-12, 2012). In this study it was shown that Lcp from *Gordonia polyisoprenivorans* VH2 (Lcp1$_{VH2}$) harbors a non-covalently bound heme *b* as cofactor, which was identified by pyridine hemochrome spectra and confirmed by LC/ESI-ToF-MS. It contains iron, most likely in the Fe^{3+} state. We focused on the characterization of the heme-cofactor, its accessibility with respect to the conformation of Lcp1$_{VH2}$, and the identification of putative histidine residues involved in the coordination of heme. A change was detectable in UV/Vis-spectra of reduced Lcp1$_{VH2}$ when imidazole was added, showing that Lcp1$_{VH2}$ "as isolated" occurs in an open state, directly being accessible for external ligands. In addition, three highly conserved histidines (H195, H200 and H228), presumably acting as ligands coordinating the heme within the heme pocket, were replaced with alanines by site-directed mutagenesis. The effect of these changes on in vivo rubber-mineralization was investigated. The *lcp*- deletion mutant complemented with the H195A variant of *lcp1*$_{VH2}$ was unable to mineralize poly(*cis*-1,4-isoprene). In vitro analyses of purified, recombinant Lcp1$_{VH2}$H195A confirmed the loss of enzyme activity, which could be ascribed to the loss of heme. Hence, H195 is essential for the association of heme-*b* in the central region of Lcp1$_{VH2}$.

Keywords *Gordonia polyisoprenivorans* strain VH2 · Latex clearing protein (Lcp) · Microbial rubber degradation · Poly(*cis*-1,4-isoprene) rubber

1 Introduction

As industrialization and human activity increasingly impact our world, the need for sustainable use of resources becomes a priority. Balanced product cycles are essential and recycling of materials is needed to reduce the amount of waste and to minimize environmental damage during production. Rubber (poly(*cis*-1,4-isoprene)) is produced in huge amounts, and even though it is a natural product, it is difficult to recycle. One recycling method that is currently being investigated is the degradation or the biotransformation of rubber by microorganisms (Yikmis and Steinbüchel 2012). Apart from a few strains like the Gram-negative bacterium *Xanthomonas* sp. 35Y (Tsuchii and Takeda 1990), mainly bacteria belonging to the actinomycetes are able to degrade rubber (Jendrossek et al. 1997). Interestingly, bacteria show two different growth patterns when cultured on rubber (Linos et al. 2000). Some bacteria form translucent halos on latex-containing mineral agar, such as strains belonging to the genus *Streptomyces* like *Streptomyces coelicolor* A3(2) or *Streptomyces* sp. K30 (Jendrossek et al. 1997; Rose et al. 2005). In contrast, other bacteria need a direct contact to the rubber material and do not form clearing zones. Representatives of these adhesively growing bacteria often belong to

Electronic supplementary material The online version of this article (https://doi.org/10.1007/s41748-018-0041-2) contains supplementary material, which is available to authorized users.

✉ Alexander Steinbüchel
steinbu@uni-muenster.de

[1] Institut für Molekulare Mikrobiologie und Biotechnologie, Westfälische Wilhelms-Universität Münster, Münster, Germany

[2] Institut für Anorganische und Analytische Chemie, Westfälische Wilhelms-Universität Münster, Münster, Germany

[3] Department of Environmental Sciences, King Abdulaziz University, Jeddah, Saudi Arabia

the order *Corynebacteriales,* such as the very potent rubber degraders of the genus *Gordonia* (Linos et al. 1999, 2000, 2002). The reasons for the different growth patterns have not been clarified, yet (Watcharakul et al. 2016). In recent years, the rubber degradation pathway of the actinobacterium *Gordonia polyisoprenivorans* VH2 has been proposed based on the genome sequence, the analysis of transposon and deletion mutants, comparative genomics, and literature search (Hiessl et al. 2012). Poly(*cis*-1,4-isoprene) is cleaved into smaller oligomers which are most likely taken up by an Mce-protein driven transport mechanism. During subsequent *β*-oxidation cycles, acetyl-CoA and propionyl-CoA are released and enter the central metabolism (Hiessl et al. 2012). The key enzyme in this pathway is the latex clearing protein (Lcp), which catalyzes the first step: the oxidation of the polymer to smaller oligomers (Fig. 1). *G. polyisoprenivorans* VH2 harbors two *lcps*, one located on the chromosome ($lcp1_{VH2}$), and one located on the plasmid p174 ($lcp2_{VH2}$). Notably, both *lcps* must be deleted to obtain a mutant unable to use poly(*cis*-1,4-isoprene) as sole carbon source (Hiessl et al. 2012). The gene $lcp1_{VH2}$ has been heterologously expressed in *E. coli,* and the protein was purified for biochemical characterization (Hiessl et al. 2014). Within that study it was shown that $Lcp1_{VH2}$ cleaved poly(*cis*-1,4-isoprene) by an endocleavage mechanism into oligomers each containing an aldehyde and a ketone functional group. An activity assay measuring the consumption of oxygen during cleavage of rubber has been established and submolar amounts of copper were detected (Hiessl et al. 2014). Subsequently, two other Lcps have been purified and characterized: Lcp_{K30} of *Streptomyces* sp. K30 and Lcp_{Rr} of *Rhodococcus rhodochrous* RPK1 (Birke et al. 2015; Watcharakul et al. 2016). 52% of the amino acid sequence of $Lcp1_{VH2}$ is identical to Lcp_{K30}, whereas 70% is identical to Lcp_{Rr} (Birke et al. 2015; Watcharakul et al. 2016). In addition to the high sequence similarity, all three Lcps share a domain of unknown function (DUF 2236). An alignment of more than 50 Lcp-similar sequences revealed three conserved histidines likely being involved in the coordination of a cofactor (Hiessl et al. 2014). A following study on Lcp_{K30} used 495 sequences similar to Lcps for an alignment (Röther et al. 2016). Based on this alignment, mutational studies showed that H198 in essential in ligand association in Lcp_{K30} (Röther et al. 2016). For Lcp_{K30} and Lcp_{Rr} heme has been identified as ligand, containing iron as metal center (Birke et al. 2015; Watcharakul et al. 2016). Nevertheless, they show differences in their color, their spectra and their conformation (Watcharakul et al. 2016). Differences in the conformation were assigned to changes in the spectra after adding imidazole to reduced Lcp (Watcharakul et al. 2016). Only recently Lcp_{K30} has been successfully crystallized and its structure solved in an "open" and a "closed" conformation, showing that it can switch between both conformations (Ilcu et al. 2017). The distal axial ligand of the heme iron shifted in the presence of imidazole, opening direct access to the heme group (Ilcu et al. 2017). Based on this knowledge, we paid in this study special emphasis to the question of cofactor and its characterization with respect to the accessibility for ligands and substrates as well as to putative amino acid residues coordinating the heme in $Lcp1_{VH2}$. The new findings will also help to gain information about commonalities of Lcps. Minor differences between Lcps (as occurred for Lcp_{K30} and Lcp_{Rr} already) can be interpreted easier in their context with new data from other Lcps.

2 Materials and Methods

2.1 Bacterial Strains, Growth Conditions, and Media

A listing of all strains, plasmids and oligonucleotides used and constructed in this work, is given in Table 1. The sequence of $lcp1_{VH2}$ can be accessed at GenBank (Benson et al. 2018) number AFA75827.1. For heterologous expression in *E. coli* C41 (DE3), the Tat-sequence was substituted by an affinity tag as previously described (Hiessl et al. 2014). Strains of *E. coli* were incubated in LB-medium at 37 °C. Precultures of *Gordonia* were grown in standard I medium and incubated at 30 °C on a rotary shaker overnight. Prior to inoculation of the mineral salt medium (MS-medium) (Schlegel et al. 1961) containing poly(*cis*-1,4-isoprene) as sole carbon source (0.2%, w/v), the cells were washed three times in sterile MS-medium. Production of the mutated $Lcp1_{VH2}$-H195A and of the wild-type $Lcp1_{VH2}$ was carried out in auto-induction medium at 30 °C (Andler and Steinbüchel 2017).

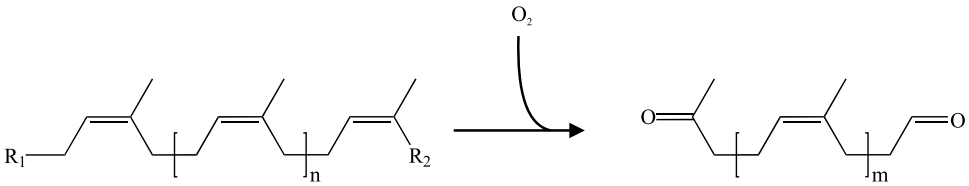

Fig. 1 Cleavage of poly(*cis*-1,4-isoprene) into oligomers catalyzed by $Lcp1_{VH2}$

Table 1 Bacterial strains, plasmids and oligonucleotides used in this study

	Description	Source or reference
Bacterial strains and plasmids		
G. polyisoprenivorans VH2	Poly(*cis*-1,4-isoprene)-degrading wild type, DSMZ 44266	Arenskötter et al. (2001)
G. polyisoprenivorans VH2-C15	*lcp1* and *lcp2* deletion mutant of *G. polyisoprenivorans* VH2; harbors apramycin and kanamycin resistance cassette	Hiessl et al. (2012)
Escherichia coli Mach1™ T1	ΔrecA1398 endA1 tonA Φ80ΔlacM15 ΔlacX74 hsdR (r_K^- m_K^+)	Invitrogen Corporation
E. coli C41 (DE3)	F^- ompT gal dcm $hsdS_B$ (r_B^- m_B^-) (DE3)	Lucigen Corporation
pJET1.2/blunt	Cloning vector, Ap^R	Thermo Fisher Scientific
pET23a(+)::His*lcp1*$_{VH2}$	Expression vector for *lcp1*$_{VH2}$, Ap^R	Hiessl et al. (2014)
pET23a(+)::His*lcp1*$_{VH2}$-H195A	Expression vector for *lcp1*$_{VH2}$ with histidine 195 substituted for alanine, Ap^R	this study
pNC9501	*E. coli—Gordonia* shuttle vector, Km^R and $Thio^R$	Matsui et al. (2006)
pNC9501::*lcp1*$_{VH2}$	*E. coli—Gordonia* shuttle vector for complementation with *lcp1*$_{VH2}$, Km^R and $Thio^R$	This study
pNC9501::*lcp1*$_{VH2}$-H195A	*E. coli—Gordonia* shuttle vector for complementation with *lcp1*$_{VH2}$-H195A, Km^R and $Thio^R$	This study
pNC9501::*lcp1*$_{VH2}$-H200A	*E. coli—Gordonia* shuttle vector for complementation with *lcp1*$_{VH2}$-H200A, Km^R and $Thio^R$	This study
pNC9501::*lcp1*$_{VH2}$-H228A	*E. coli—Gordonia* shuttle vector for complementation with *lcp1*$_{VH2}$-H228A, Km^R and $Thio^R$	This study
Oligonucleotides		
1Lcp1VH2H195A	CGGATGGCCGCTGCGGGTGTGC	This study
2Lcp1VH2H195A	GCACACCCGCAGCGGCCATCCG	This study
1Lcp1VH2H200A	GGTGTGCGGGCTCTGCTGCCC	This study
2Lcp1VH2H200A	GGGCAGCAGAGCCCGCACACC	This study
1Lcp1VH2H228A	GGTCACCTGGGCCAGTCTGCCG	This study
2Lcp1VH2H228A	CGGCAGACTGGCCCAGGTGACC	This study
1Lcp1VH2_Promotor_EcoRI	AAAGAATTCCTGCTGGGCGATGAACTGTGC	This study
4Lcp1VH2_Stop_EcoRI	AAAGAATTCTCAGTTGTAGTTCGGGTTGTTGAAGTAGGG	This study

Abbreviations for *Escherichia coli* genotypes from Berlyn (1998). *Ap^R* ampicillin resistant, *Km^R* kanamycin resistant, *$Thio^R$* thiostrepton resistant

2.2 Chemicals and Oligonucleotides

Chemicals used in this study were obtained from Sigma-Aldrich Chemie GmbH (Steinheim, Germany) and Carl Roth GmbH & Co. KG (Karlsruhe, Germany), respectively. Synthetic poly(*cis*-1,4-isoprene) (CAS no. 104389-31-3) for mineralization experiments was cryomilled as described before (Hiessl et al. 2012; Warneke et al. 2007). Latex milk (Neotex Latz; CAS no. 9006-04-06), was obtained from Weber & Schaer GmbH & Co. KG (Hamburg, Germany). Ammonia was separated from the latex milk by centrifugation at 10,000×*g* for 10 min. The solid top latex layer was removed, and the liquid middle latex layer was 1:5 diluted before it was used for oxygen consumption assays; ammonia remained at the bottom (Hiessl et al. 2014). Oligonucleotides were purchased from Eurofins Genomics GmbH (Ebersberg, Germany).

2.3 Purification of Lcp1$_{VH2}$ and Lcp1$_{VH2}$-H195A

Lcp1$_{VH2}$ and Lcp1$_{VH2}$-H195A were purified with a His-tag as described previously (Hiessl et al. 2014) or with a Strep-tactin-tag if it was subsequently used for metal analysis employing a kit from IBA Lifesciences GmbH (Göttingen, Germany). If necessary, the concentration of Lcp1$_{VH2}$ was increased after purification by a Vivaspin®-column with a volume of 500 µl–6 ml and a molecular weight cut off of 10,000 Da (Sartorius AG, Göttingen, Germany). Further characterization experiments were carried out in buffer containing 200 mM Tris at pH 7.4. The amounts of protein obtained were measured by the dye-ligand assay according to Bradford (1976).

2.4 Oxygen Consumption Assay

The oxygen consumed by $Lcp1_{VH2}$ during cleavage of poly(*cis*-1,4-isoprene) was monitored by the Digital Model 20 oxygen measurement controller of Rank Brothers Ltd (Cambridge, UK). The cell was set up and calibrated according to the manufacturer's manual. 10 µg/ml purified protein and 20 µl/ml of a 20% latex emulsion were incubated in 200 mM Bis–Tris buffer (pH 7.4). Activity was measured at 23 °C, and the consumption was recorded by a PicoLog 1216 data logger combined with the PicoLog software from Pico Technology (Cambridgeshire, UK).

2.5 TXRF-Analysis for Identification of Metal Cofactors

Total reflection X-ray Fluorescence (TXRF) analysis of $Lcp1_{VH2}$ was performed using an S2 PICOFOX system (Bruker AXS, Berlin, Germany) with a low power X-ray tube with a molybdenum anode and an energy-dispersive, Peltier-cooled silicon drift detector XFlash (Bruker AXS, Berlin, Germany). 100 µl of the sample solution ($Lcp1_{VH2}$ in 0.2 M Bis–Tris buffer; pH 7.0) were mixed with the same volume of the internal arsenic standard [c(As) = 10 µg/ml in 20% HNO_3]. 5 µl of this solution were placed on the sample carriers (quartz glass) and dried via evaporation. Excitation settings were 50 kV and 750 µA. Measurements were performed by signal integration over 1000 s and data evaluated using the software SPECTRA version 6.1.5.0 (Bruker AXS, Berlin, Germany).

2.6 Detection of Non-covalently Bound Heme-*b*

SDS-gels and native gels were stained by the method of Thomas et al. (1976) with changes described by Goodhew et al. (1986) to detect a heme pseudoperoxidase activity of $Lcp1_{VH2}$. The type of heme was determined with pyridine hemochrome spectra (Berry and Trumpower 1987). For comparison, changes were applied as described by Birke et al. (2015).

The LC/ESI-ToF–MS investigations were carried out using an Alexys LC100 high-performance liquid chromatography system (Antec Leyden, Zoeterwoude, The Netherlands). This LC system consisted of two LC 100 pumps, an AS100 autosampler, a Decade II column oven and an AC100 controller. The LC outlet was coupled to an electrospray ionization (ESI) source of a time-of-flight mass spectrometer, model micrOTOF from Bruker Daltonics (Bremen, Germany). Mass spectra were recorded in the positive ESI mode using the full scan mode in a mass range from *m/z* 100–2200. The following parameters were used for all measurements: end plate offset: −500 V, capillary: −4000 V, nebulizer gas: 1.5 bar, dry gas: 9 l/min, dry temperature: 200 °C, capillary exit: 150.0 V, skimmer 1: 50.0 V, skimmer 2: 26.5 V, hexapole 1: 23.0 V, hexapole 2: 21.4 V, hexapole RF: 350.0 V, transfer time: 70.0 ms, pre-pulse storage: 19 ms, lens 1 storage: 40 V, lens 1 extraction: 20.9 V. The instrument was routinely calibrated using ammonium formate clusters as external standards. Furthermore, at the beginning of each data acquisition, internal mass calibration was performed using ammonium formate clusters as well. The software DataAnalysis from Bruker Daltonics was used for spectra evaluation. The acquired protein mass spectra with characteristic charge distributions were deconvoluted to obtain neutral mass spectra for a clearer understanding. A Discovery BioWidePore C5 column (2.1 × 100 mm, 3 µm, 300 Å) from Supelco (Steinheim, Germany) was used for all separations. The injection volume was 5 µl from 10 µM $Lcp1_{VH2}$ in 10 mM ammonium acetate, and the column oven had a temperature of 40 °C. Separation was performed using a flow rate of 300 µl/min and a binary gradient with eluent A as aqueous 0.1% formic acid and eluent B as acetonitrile. The gradient started at 20% B for 2 min, then rising within 10 min to 70%. It was held at 70% for 3 min followed by a decrease in 3 min back to 20% and was held at 20% for 2 min resulting in a total run time of 20 min, respectively.

2.7 Site Directed Mutagenesis

Histidines were substituted for alanines using site directed mutagenesis as described by Laible and Boonrod (2009). Changes were applied as follows. For amplification of the plasmids, a Phusion® High-Fidelity DNA polymerase (Thermo Fisher Scientific, Waltham, USA) was used. Primers containing the desired mutations are listed in Table 1. After amplification and purification of the whole vector, methylated template DNA was digested with 2 µl *Dpn*I. DNA obtained by PCR was non-methylated and contained the designed mutation. In comparison, template plasmid containing the original sequence was methylated and thus recognized and digested by *Dpn*I. Competent cells of *E. coli* Mach1™T1 were transformed by the method described by Hanahan (1983), grown with a selecting antibiotic, and plasmids isolated from the overnight-grown culture with the GeneJET Plasmid Miniprep Kit (Thermo Scientific, Waltham, USA) according to the manual.

2.8 Complementation of *G. polyisoprenivorans* VH2-C15 and Mineralization of Polyisoprene

The *E. coli-Gordonia* shuttle vector pNC9501 (Matsui et al. 2006) was used for complementing the *lcp*-double deletion mutant *G. polyisoprenivorans* VH2-C15 (Hiessl et al. 2014) with variants of $lcp1_{VH2}$. The region 605 bp upstream of $lcp1_{VH2}$ was also cloned to the vector, to ensure that the expression of $lcp1_{VH2}$ was regulated by the native promoter.

The phenotypic effect of the mutations was monitored by measuring the mineralization of poly(*cis*-1,4-isoprene) (Ibrahim et al. 2006). Tightly closed Erlenmeyer flasks contained 100 ml MS-medium inoculated with a well-grown preculture and 0.2% (w/v) poly(*cis*-1,4-isoprene). In addition, a test tube filled with 15 ml of 0.2 M $Ba(OH)_2$ was inserted into each flask. $Ba(OH)_2$ was used to precipitate the CO_2 formed during the cultivation as $BaCO_3$. At each measurement point, the test tubes were replaced by tubes containing fresh $Ba(OH)_2$-solution, and the flasks were aerated. The amount of CO_3^{2-} formed was determined by titration of the remaining $Ba(OH)_2$ with HCl in comparison to a control containing MSM and poly(*cis*-1,4-isoprene) without cells. As pH indicator, 20 µl phenolphthalein (1%, w/v, in isopropanol) was added, and titration was performed until the solution became colorless. The mineralization of poly(*cis*-1,4-isoprene) given in $\%CO_2$, was calculated with the following equation.

$$\text{Mineralization}\ (\%CO_2) = \frac{\text{Concentration of HCl}\left(\frac{\text{mol}}{\text{ml}}\right) \times \text{Required amount of HCl (ml)} \times 100\%}{\text{C} - \text{content of amount of poly}(cis{-}1,4\text{ - isoprene})\text{applied (mol)} \times 2}$$

3 Results

3.1 Iron is the Only Metal Detected in $Lcp1_{VH2}$

Employing a sensitive TXRF analysis revealed iron as the only metal in $Lcp1_{VH2}$ when the enzyme was purified with a Strep-tag. The state of the iron atom has been confirmed to be Fe^{3+} by a characteristic oxidized spectrum and by a spectrum which did not change after treatment with CO (Supplemental Fig. 1).

3.2 The Cofactor of $Lcp1_{VH2}$ is Heme of a *b*-type

The UV/Vis-spectrum of $Lcp1_{VH2}$ obtained directly after isolation and without any further treatment ("as isolated") showed a characteristic peak at 412 nm (Fig. 2). This absorption maximum was first assigned to the maximum at about 420 nm of copper containing white laccases (Hiessl et al. 2014). Nevertheless, this maximum (Soret band) is also characteristic for proteins containing a heme-group. To elucidate whether the peak appears in a spectrum of $Lcp1_{VH2}$ due to a heme-group, the spectrum was further analyzed. We reduced $Lcp1_{VH2}$ with dithionite and observed not only a shift of the Soret band to 430 nm, but also the appearance of a $Q_{0.1}$-band at 533 nm and a broad $Q_{0.0}$-band at 558–564 nm (Fig. 2). This spectrum of reduced $Lcp1_{VH2}$ corresponds to spectra of reduced heme-containing proteins. Another indication for the presence of heme was the confirmation of an $Lcp1_{VH2}$-mediated peroxidase activity after incubation of native gels in 3,3′,5,5′-tetramethylbenzidine (TMB)-solution with H_2O_2. When TMB gets oxidized during the reaction, it forms a product with blue color. The band at the height of $Lcp1_{VH2}$ turned blue, while under denaturing conditions (SDS-gel), no band corresponding to the size of $Lcp1_{VH2}$ became visible (Supplemental Fig. 2). This suggests the presence of a non-covalently bound heme. Accordingly, we identified the heme type with a pyridine hemochrome spectrum (Fig. 3a). By performing the assay, between heme-*b* and heme-*c* can be distinguished due to absorbance at different wavelengths. Heme-*b* absorbs light at 556.4 nm and heme-*c* at 549.9 nm. Here we used cytochrome *c* and myoglobin as controls for heme-*c* and heme-*b* containing proteins, respectively. $Lcp1_{VH2}$ showed a characteristic absorbance-peak for heme-*b* of 556 nm. Subsequent LC/

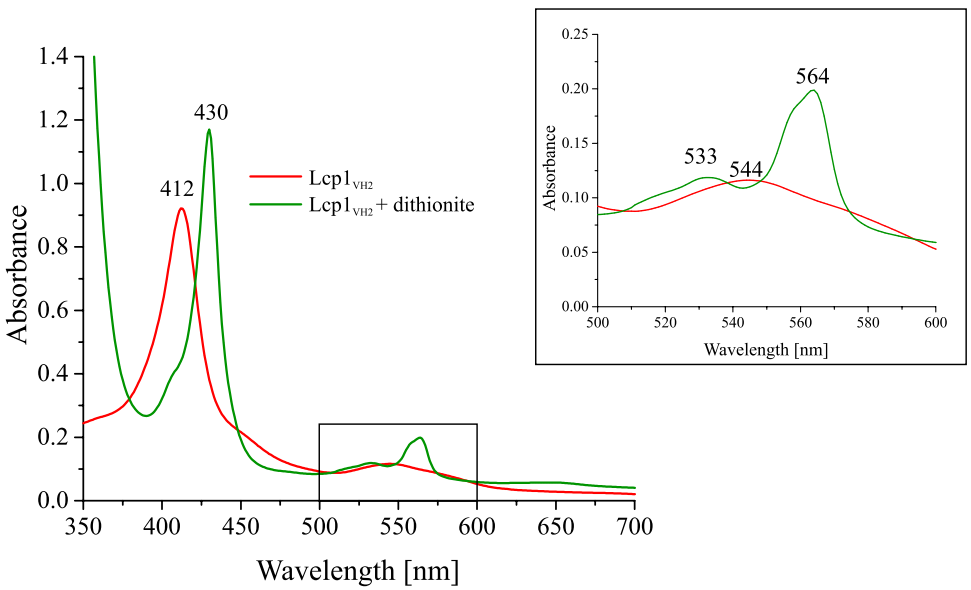

Fig. 2 UV/Vis-spectra of $Lcp1_{VH2}$ in the states as-isolated (red) and reduced with dithionite (green). The bands at 412 nm (Soret band) and 544 nm (*Q*-band) of the as-isolated state as well as their shift to 430 nm and 533 nm in the reduced state, are characteristic for heme spectra and similar to those of Lcp_{K30} and Lcp_{Rr}. The $Q_{0.0}$-band (558–564) appears in broad band in $Lcp1_{VH2}$

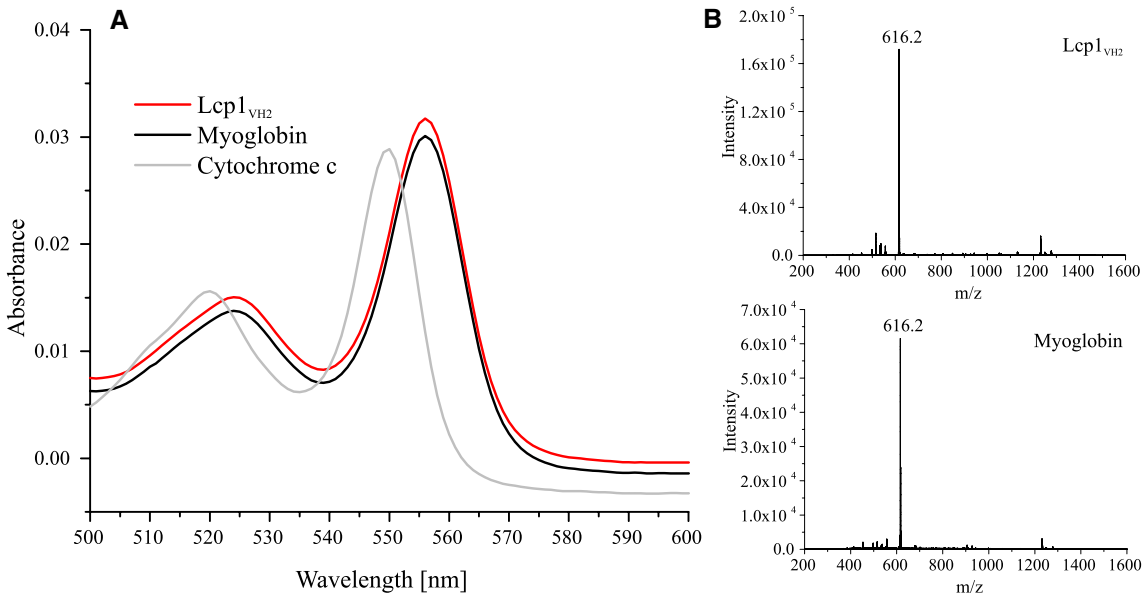

Fig. 3 Determination of the heme-type in $Lcp1_{VH2}$ (red; upper mass spectrum) by pyridine hemochrome spectrum (**a**) and LC/ESI-ToF–MS (**b**). Myoglobin (black; lower mass spectrum) and cytochrome *c* (grey) served as controls

ESI-ToF–MS analysis confirmed the presence of heme-*b*. The detected mass of 616.2 Da perfectly accords with the mass of heme-*b* and the myoglobin control (Fig. 3b). The appearance of a mass of 616.2 Da separated from $Lcp1_{VH2}$ (43.8 kDa) demonstrates the dissociation during liquid chromatography due to the non-covalent binding of the heme.

3.3 Open Conformation of $Lcp1_{VH2}$

Lcp can occur in two different conformations: an open and a closed state (Ilcu et al. 2017; Watcharakul et al. 2016). When imidazole is added to a reduced Lcp of an open state, a change in the spectrum is observable due to the binding of imidazole to the reduced heme group. In contrast, imidazole cannot access to the heme group if Lcp rests in a closed state (Watcharakul et al. 2016). The conformation of $Lcp1_{VH2}$ seems to be an open conformation, since the addition of imidazole to reduced $Lcp1_{VH2}$ resulted in a change of the spectrum (Fig. 4). The *Q*-bands increased when 1 mM imidazole was added. Not only imidazole had an impact on the spectrum of $Lcp1_{VH2}$, but also the treatment with mercaptoethanol resulted in a change (Supplemental Fig. 3).

3.4 Histidine 195 is Essential for the Heme Binding in $Lcp1_{VH2}$

Histidines are known to associate heme in proteins. An alignment performed by Hiessl et al. using more than 50 whole amino acid sequences of Lcp-similar proteins revealed three highly conserved histidine residues (Hiessl et al. 2014). In $Lcp1_{VH2}$, they are located at position 195, 200 and 228.

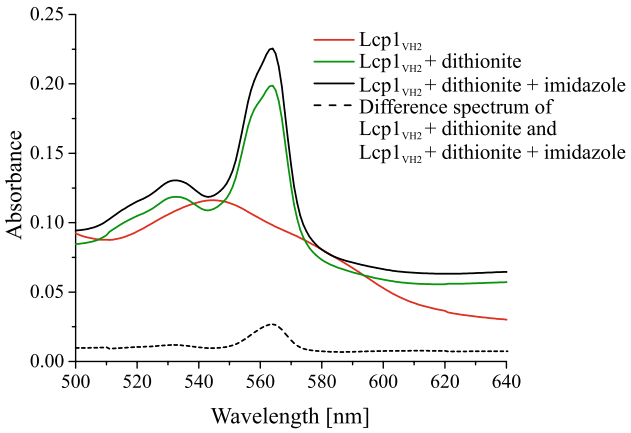

Fig. 4 UV/Vis-spectrum of $Lcp1_{VH2}$ (red) after addition of dithionite (green) and imidazole (black). Marked in a dashed line is the difference spectrum of $Lcp1_{VH2}$ with addition of dithionite and the spectrum with additional imidazole (1 mM). The spectra were monitored in 200 mM tris-buffer at room temperature

By site directed mutagenesis, we substituted all three histidines for alanines and cloned the *lcp*-variants together with 605 bp upstream of $lcp1_{VH2}$ into the *E. coli-Gordonia* shuttle vector pNC9501 (Table 1). The double deletion mutant *G. polyisoprenivorans* VH2-C15 (Hiessl et al. 2012) was transformed with the vector pNC9501::$lcp1_{VH2}$ as well as histidine-substituted variants. Resulting mutants were incubated with 0.2% (w/v) poly(*cis*-1,4-isoprene), and its capability to mineralize poly(*cis*-1,4-isoprene) was monitored (Fig. 5). *G. polyisoprenivorans* VH2 and VH2-C15 without plasmid were used as controls. About 27% of

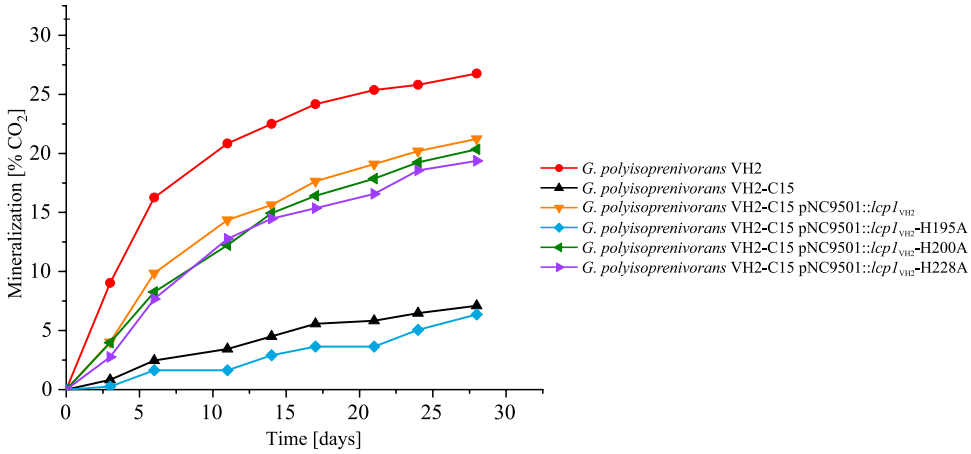

Fig. 5 Mineralization of poly(*cis*-1,4-isoprene) by strains of *G. polyisoprenivorans* VH2-C15 complemented with plasmids containing *lcp1*$_{VH2}$ variants. 500 ml flasks containing 100 ml MSM and 0.2% (w/v) poly(*cis*-1,4-isoprene) were incubated on a rotary shaker at 30 °C and aerated twice a week. Mineralization was determined as described in "Materials and methods". For complementation, *lcp1*$_{VH2}$ and variants were ligated to the vector pNC9501

poly(*cis*-1,4-isoprene) were mineralized to CO_2 by the wild-type (*G. polyisoprenivorans* VH2). Additional carbon, which is taken up during the degradation of polyisoprene, is used to generate biomass. The complemented mutants were able to mineralize about 20% of the polymer. Interestingly, the mutant with His195-substitution did not mineralize poly(*cis*-1,4-isoprene). Slight CO_2 formation of ~ 6% was observed as well for the double deletion mutant VH2-C15 and may be caused by lysis of cells. To ensure the deficiency was caused by a change of the heme-binding, *lcp1*$_{VH2}$-H195A was heterologously expressed in *E. coli* C41(DE3). Since the yield of Lcp1$_{VH2}$-H195 was low with IPTG-induced LB-medium, we used an auto-induction medium as described earlier (Andler and Steinbüchel 2017). Consistently, we expressed *lcp1*$_{VH2}$ in auto-induction medium to maintain comparability and to exclude differences caused by different methods. After purification, Lcp1$_{VH2}$-H195A clearly showed no coloration, while Lcp1$_{VH2}$ remained red. This observation was the first sign of a change in heme-binding. The finding was confirmed by a spectrum, where neither a Soret band at 412 nm, nor a slight increase at 544 nm was detected, which were both present in the wild-type Lcp1$_{VH2}$ and are characteristic for heme proteins (Fig. 6a). Further, Lcp1$_{VH2}$-H195A did not show any activity, when the oxygen consumption was measured (Fig. 6b).

4 Discussion

In a previous study, copper was detected in purified Lcp1$_{VH2}$ (Hiessl et al. 2014). Since in Lcp$_{K30}$ and Lcp$_{Rr}$ iron was detected as cofactor, the question arose whether the hexahistidine-tag could promote unspecific interaction with copper. Therefore, we used Strep-tagged Lcp1$_{VH2}$ for sensitive TXRF-analysis in this study. No copper, but iron was detected as cofactor of Lcp1$_{VH2}$, which is in good agreement

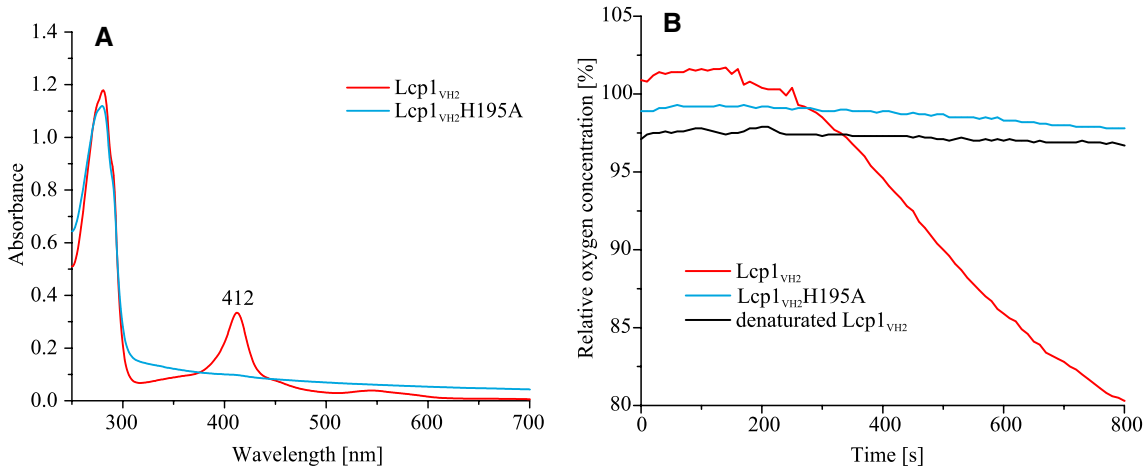

Fig. 6 Activity (**a**) and UV/Vis-spectrum (**b**) of Lcp1$_{VH2}$ (red) compared to Lcp1$_{VH2}$-H195A (blue). The activity was measured by consumption of oxygen with an oxygen electrode in 200 mM Bis–Tris-buffer at pH 7.4 (10 µg Lcp1$_{VH2}$)

with findings obtained for similar Lcps and further results confirming heme in $Lcp1_{VH2}$ (Birke et al. 2015; Watcharakul et al. 2016). Nevertheless, the detection of metals in Lcps remains challenging. For Lcp_{Rr} in addition to iron copper was found in submolar concentrations during the metal analysis (Watcharakul et al. 2016).

All hitherto isolated Lcps ($Lcp1_{VH2}$, Lcp_{K30} and Lcp_{Rr}) (1) share a high sequence homology, (2) cleave rubber with an endocleavage mechanism, and (3) contain heme-*b* as cofactor (Birke et al. 2015; Hiessl et al. 2014; Watcharakul et al. 2016). Nevertheless, differences between Lcp_{K30} and Lcp_{Rr} have previously been reported (Birke et al. 2015; Watcharakul et al. 2016). The main, directly observed difference was the brownish color of Lcp_{Rr} instead of the red color of concentrated Lcp_{K30}-solutions (Watcharakul et al. 2016). An additional broad absorption maximum around 645 nm was given as explanation for the observed brown color. Main absorption maxima at 412 and 544 nm for Lcp_{K30} were present in Lcp_{Rr}, but peaked at slightly different wavelengths of 407 and 535 nm. Remarkably, differences appeared in the *Q*-bands, when the reduced spectra of both Lcps were analyzed. The *Q*-bands of Lcp_{Rr} were considerably less prominent when compared to Lcp_{K30}. Another difference appeared in the dithionite-reduced spectrum, when imidazole was added. The influence of an external ligand (in this case imidazole) on the accessibility of the heme group has been shown for Lcp_{K30} in the crystal structure (Ilcu et al. 2017). As imidazole did not influence the spectrum of dithionite-reduced Lcp_{K30}, it was postulated that Lcp_{K30} rests in a sixfold coordinated "closed" state, without accessibility for external ligands. In contrast, a considerable increase of the *Q*-bands was detected in Lcp_{Rr} when imidazole was added (Watcharakul et al. 2016). This increase was explained by the binding of imidazole to the reduced heme, which implied that Lcp_{Rr} was accessible to external ligands or substrates in an "open" state (fivefold coordinated) (Watcharakul et al. 2016).

Interestingly, when characteristics of $Lcp1_{VH2}$ are compared with those of Lcp_{K30} and Lcp_{Rr}, the enzyme does not seem to be more or less similar to one or the other. It shares some communalities with Lcp_{K30} and some with Lcp_{Rr}. With respect to the UV/Vis-absorbance in either state ("as isolated" or reduced), $Lcp1_{VH2}$ shows the same spectrum as Lcp_{K30}. The Q-band at 562 nm was detected in both, albeit in $Lcp1_{VH2}$ the band has a broader range, which does not display a major difference (Birke et al. 2015). The broad peak could be the beginning of a split Q-band; a known phenomenon for which different reasons have been postulated (Reddy et al. 1996). It might be induced by the surrounding of the heme pocket, but a more precise explanation can so far not be given. Similar to Lcp_{K30}, $Lcp1_{VH2}$ does not exhibit any additional peaks, and concentrated samples are red-colored (Hiessl et al. 2014). However, the conformation of $Lcp1_{VH2}$ "as isolated", was in open state, as suggested by spectral changes after addition of imidazole and mercaptoethanol. Lcp_{K30}, in contrast was "as isolated" found in closed state (Watcharakul et al. 2016). Interestingly, in this case $Lcp1_{VH2}$ and Lcp_{Rr} share the fivefold coordinated open state. Watcharakul et al. (2016) postulated that the open state might correlate with the less pronounced *Q*-bands of Lcp_{Rr}. This does not apply to $Lcp1_{VH2}$, which has characteristic *Q*-bands, similar to those found in Lcp_{K30}, and no 645 nm peak. Taking not only a look on the protein level, but the phylogenetic relation and the growth pattern on rubber of the strains, one notices the close relation between *R. rhodochrous* and *G. polyisoprenivorans*. Both bacteria exhibited adhesive growth with poly(*cis*-1,4-isoprene), while *Streptomyces* sp. K30 forms clearing zones. Watcharakul et al. (2016) hypothesized that adhesively growing bacteria harbor Lcp in open conformation, which is accessible to external ligands and substrates without conformational change. The results obtained in this work seem to reinforce this hypothesis, since the adhesively growing strain *G. polyisoprenivorans* VH2 contains an Lcp in open conformation as well. Still, the hypothesis cannot be supported, because $Lcp1_{VH2}$ prompts *Streptomyces lividans* TK23 to form translucent halos, while its natural host *G. polyisoprenivorans* VH2 grows adhesively (Bröker et al. 2008). *S. lividans* TK23 is not able to grow on rubber, but when complemented with $lcp1_{VH2}$, clear-zones on latex overlay-agar plates became visible (Bröker et al. 2008). Accordingly, the conformation of Lcp does not influence the growth behavior on rubber. Another explanation for the difference in growth behavior is the occurrence of mycolic acids (Linos et al. 2000). To the best of our knowledge, this hypothesis is still in agreement with the growth pattern observed in new isolates. The previously isolated *R. rhodochrous* RPK1 is likely to contain mycolic acids, like other strains of this species. Furthermore, it has been shown that the adhesion of bacteria with mycolic acids is favored on hydrophobic surfaces (Bendinger et al. 1993) such as polyisoprene.

Lcps contain a domain of unknown function (DUF2236; Pfam accession no. PF09995). Within this domain, three histidines are highly conserved as observed, when Lcps are aligned and compared as performed by Hiessl et al. (2014). In $Lcp1_{VH2}$ the histidines are located at positions 195, 200 and 228. All three histidines were replaced with alanines by site directed mutagenesis. Complementing the double deletion mutant *G. polyisoprenivorans* VH2-C15 (Hiessl et al. 2012) with $lcp1_{VH2}$ and the variants created, we have shown in vivo that the exchange of H195 with alanine results in the inability to mineralize rubber. Therefore, $lcp1_{VH2}$-H195A was heterologously expressed in *E. coli* and the corresponding protein purified and analyzed. As it showed no coloration, no activity and no characteristic peaks for a heme-containing protein, it was concluded that heme could no longer

be incorporated into the enzyme. In Lcp_{K30}, the analogous histidine 195 is located at position 198. It has been reported that the exchange of this amino acid also led to the loss of heme (Röther et al. 2016). These findings are in agreement with those that histidine is one axial ligand of the heme-group in both Lcps. The crystal structure of Lcp_{K30} confirmed H198 as axial ligand of the heme cofactor in Lcp_{K30} (Ilcu et al. 2017). A 3D-model of $Lcp1_{VH2}$ (Supplemental Fig. 4) has been generated using the Swissmodel software (Arnold et al. 2006). As the crystal structure of Lcp_{K30} is hitherto the only structure of Lcps available, it needs to be taken into account that the model is generated on this basis only. Thus, $Lcp1_{VH2}$ resembles Lcp_{K30} in this model. After all, the model supports the finding that H195 is a ligand of the heme cofactor (Supplemental Fig. 4B).

In conclusion, this study clarified that $Lcp1_{VH2}$ contains iron as the central atom of heme-*b*. Reduced enzyme activity with 1,10-phenanthroline and 2,2-bipyridyl as iron chelators support this finding (Hiessl et al. 2014). The identification of heme-*b* is also in agreement with the results published for Lcp_{K30} and Lcp_{Rr} (Birke et al. 2015; Watcharakul et al. 2016). We further examined the heme-cofactor of $Lcp1_{VH2}$ on the basis of its accessibility for ligands and its coordination within the protein. The importance of conserved histidines in Lcp was analyzed in vivo. The mineralization studies showed that histidine at position 195 is essential for strain VH2 to use rubber as sole source of carbon and energy, and in vitro it was confirmed that this deficiency depends on the lack of heme-association.

Acknowledgements The support by Weber & Schaer GmbH & Co. KG (Hamburg, Germany) by providing polyisoprene (Neotex Latz) is gratefully acknowledged. Financial support of this project by the Deutsche Forschungsgemeinschaft is very much appreciated.

Compliance with Ethical Standards

Conflict of interest On behalf of all authors, the corresponding author states that there is no conflict of interest.

References

Andler R, Steinbüchel A (2017) A simple, rapid and cost-effective process for production of latex clearing protein to produce oligopolyisoprene molecules. J Biotechnol 241:184–192. https://doi.org/10.1016/j.jbiotec.2016.12.008

Arenskötter M, Baumeister D, Berekaa M, Pötter G, Kroppenstedt RM, Linos A, Steinbüchel A (2001) Taxonomic characterization of two rubber degrading bacteria belonging to the species *Gordonia polyisoprenivorans* and analysis of hyper variable regions of 16S rDNA sequences. FEMS Microbiol Lett 205:277–282. https://doi.org/10.1016/S0378-1097(01)00497-9

Arnold K, Bordoli L, Kopp J, Schwede T (2006) The SWISS-MODEL workspace: a web-based environment for protein structure homology modelling. Bioinformatics 22:195–201. https://doi.org/10.1093/bioinformatics/bti770

Bendinger B, Rijnaarts HHM, Altendorf K, Zehnder AJB (1993) Physicochemical cell surface and adhesive properties of coryneform bacteria related to the presence and chain length of mycolic acids. Appl Environ Microbiol 59:3973–3977

Benson DA, Cavanaugh M, Clark K, Karsch-Mizrachi I, Ostell J, Pruitt KD, Sayers EW (2018) GenBank. Nucleic Acids Res 46:D41–D47. https://doi.org/10.1093/nar/gkx1094

Berlyn MKB (1998) Linkage map of *Escherichia coli* K-12, edition 10: the traditional map. Microbiol Mol Biol Rev 62:814–984

Berry EA, Trumpower BL (1987) Simultaneous determination of hemes *a*, *b*, and *c* from pyridine hemochrome spectra. Anal Biochem 161:1–15. https://doi.org/10.1016/0003-2697(87)90643-9

Birke J, Röther W, Jendrossek D (2015) Latex clearing protein (Lcp) of *Streptomyces* sp. strain K30 is a *b*-type cytochrome and differs from rubber oxygenase A (RoxA) in its biophysical properties. Appl Environ Microbiol 81:3793–3799. https://doi.org/10.1128/AEM.00275-15

Bradford MM (1976) A rapid and sensitive method for the quantitation of microgram quantities of protein utilizing the principle of protein-dye binding. Anal Biochem 72:248–254. https://doi.org/10.1016/0003-2697(76)90527-3

Bröker D, Dietz D, Arenskötter M, Steinbüchel A (2008) The genomes of the non-clearing-zone-forming and natural-rubber-degrading species *Gordonia polyisoprenivorans* and *Gordonia westfalica* harbor genes expressing Lcp activity in *Streptomyces* strains. Appl Environ Microbiol 74:2288–2297. https://doi.org/10.1128/AEM.02145-07

Goodhew CF, Brown KR, Pettigrew GW (1986) Haem staining in gels, a useful tool in the study of bacterial *c*-type cytochromes. BBA Bioenergetics 852:288–294. https://doi.org/10.1016/0005-2728(86)90234-3

Hanahan D (1983) Studies on transformation of *Escherichia coli* with plasmids. J Mol Biol 166:557–580. https://doi.org/10.1016/S0022-2836(83)80284-8

Hiessl S et al (2012) Involvement of two latex-clearing proteins during rubber degradation and insights into the subsequent degradation pathway revealed by the genome sequence of *Gordonia polyisoprenivorans* strain VH2. Appl Environ Microbiol 78:2874–2887. https://doi.org/10.1128/AEM.07969-11

Hiessl S, Böse D, Oetermann S, Eggers J, Pietruszka J, Steinbüchel A (2014) Latex clearing protein-an oxygenase cleaving poly(*cis*-1,4-isoprene) rubber at the *cis* double bonds. Appl Environ Microbiol 80:5231–5240. https://doi.org/10.1128/AEM.01502-14

Ibrahim EMA, Arenskötter M, Luftmann H, Steinbüchel A (2006) Identification of poly(*cis*-1,4-isoprene) degradation intermediates during growth of moderately thermophilic actinomycetes on rubber and cloning of a functional *lcp* homologue from *Nocardia farcinica* strain E1. Appl Environ Microbiol 72:3375–3382. https://doi.org/10.1128/AEM.72.5.3375-3382.2006

Ilcu L, Röther W, Birke J, Brausemann A, Einsle O, Jendrossek D (2017) Structural and functional analysis of latex clearing protein (Lcp) provides insight into the enzymatic cleavage of rubber. Sci Rep 7:6179. https://doi.org/10.1038/s41598-017-05268-2

Jendrossek D, Tomasi G, Kroppenstedt RM (1997) Bacterial degradation of natural rubber: a privilege of actinomycetes? FEMS Microbiol Lett 150:179–188. https://doi.org/10.1016/S0378-1097(97)00072-4

Laible M, Boonrod K (2009) Homemade site directed mutagenesis of whole plasmids. J Vis Exp. https://doi.org/10.3791/1135

Linos A, Steinbüchel A, Spröer C, Kroppenstedt RM (1999) *Gordonia polyisoprenivorans* sp. nov., a rubber-degrading actinomycete isolated from an automobile tyre. Int J Syst Bacteriol 49:1785–1791

Linos A et al (2000) Biodegradation of *cis*-1,4-polyisoprene rubbers by distinct actinomycetes: microbial strategies and detailed surface

analysis. Appl Environ Microbiol 66:1639–1645. https://doi.org/10.1128/AEM.66.4.1639-1645.2000

Linos A, Berekaa MM, Steinbüchel A, Kim KK, Spröer C, Kroppenstedt RM (2002) *Gordonia westfalica* sp. nov., a novel rubber-degrading actinomycete. Int J Syst Evol Microbiol 52:1133–1139. https://doi.org/10.1099/ijs.0.02107-0

Matsui T, Saeki H, Shinzato N, Matsuda H (2006) Characterization of *Rhodococcus-E. coli* shuttle vector pNC9501 constructed from the cryptic plasmid of a propene-degrading bacterium. Curr Microbiol 52:445–448. https://doi.org/10.1007/s00284-005-0237-1

Reddy KS, Angiolillo PJ, Wright WW, Laberge M, Vanderkooi JM (1996) Spectral splitting in the α ($Q_{0,0}$) absorption band of ferrous cytochrome *c* and other heme proteins. Biochemistry 35:12820–12830. https://doi.org/10.1021/bi960895l

Rose K, Tenberge KB, Steinbüchel A (2005) Identification and characterization of genes from *Streptomyces* sp. strain K30 responsible for clear zone formation on natural rubber latex and poly(*cis*-1,4-isoprene) rubber degradation. Biomacromol 6:180–188. https://doi.org/10.1021/bm0496110

Röther W, Austen S, Birke J, Jendrossek D (2016) Cleavage of rubber by the latex clearing protein (Lcp) of *Streptomyces* sp. strain K30: molecular insights. Appl Environ Microbiol 82:6593–6602. https://doi.org/10.1128/AEM.02176-16

Schlegel HG, Kaltwasser H, Gottschalk G (1961) Ein submersverfahren zur kultur wasserstoffoxydierender bakterien: wachstumsphysiologische untersuchungen. Arch Microbiol 38:209–222. https://doi.org/10.1007/BF00422356

Thomas PE, Ryan D, Levin W (1976) An improved staining procedure for the detection of the peroxidase activity of cytochrome P-450 on sodium dodecyl sulfate polyacrylamide gels. Anal Biochem 75:168–176. https://doi.org/10.1016/0003-2697(76)90067-1

Tsuchii A, Takeda K (1990) Rubber-degrading enzyme from a bacterial culture. Appl Environ Microbiol 56:269–274

Warneke S, Arenskötter M, Tenberge KB, Steinbüchel A (2007) Bacterial degradation of poly(*trans*-1,4-isoprene (gutta percha). Microbiology (SGM) 153:347–356. https://doi.org/10.1099/mic.0.2006/000109-0

Watcharakul S, Röther W, Birke J, Umsakul K, Hodgson B, Jendrossek D (2016) Biochemical and spectroscopic characterization of purified Latex Clearing Protein (Lcp) from newly isolated rubber degrading *Rhodococcus rhodochrous* strain RPK1 reveals novel properties of Lcp. BMC Microbiol 16:92. https://doi.org/10.1186/s12866-016-0703-x

Yikmis M, Steinbüchel A (2012) Historical and recent achievements in the field of microbial degradation of natural and synthetic rubber. Appl Environ Microbiol 78:4543–4551. https://doi.org/10.1128/AEM.00001-12